Tu et al. *Zool. Res.* 2023, 44(2): 331−340
https://doi.org/10.24272/j.issn.2095-8137.2022.356

ZR | Zoological Research

Article Open Access

C9orf72 poly-GA proteins impair neuromuscular transmission

Wen-Yo Tu[1,#], Wentao Xu[1,#], Jianmin Zhang[1], Shuyuan Qi[1], Lei Bai[1], Chengyong Shen[1,2,*], Kejing Zhang[1,*]

[1] *Zhejiang Provincial Key Laboratory of Pancreatic Disease*, *Department of Neurobiology*, *First Affiliated Hospital*, *Institute of Translational Medicine*, *School of Medicine*, *Zhejiang University*, *Hangzhou*, *Zhejiang* 310020, *China*

[2] *MOE Frontier Science*, *Center for Brain Research and Brain-Machine Integration*, *Zhejiang University*, *Hangzhou*, *Zhejiang* 310058, *China*

ABSTRACT

Amyotrophic lateral sclerosis (ALS) is a devastating motoneuron disease, in which lower motoneurons lose control of skeletal muscles. Degeneration of neuromuscular junctions (NMJs) occurs at the initial stage of ALS. Dipeptide repeat proteins (DPRs) from G4C2 repeat-associated non-ATG (RAN) translation are known to cause C9orf72-associated ALS (C9-ALS). However, DPR inclusion burdens are weakly correlated with neurodegenerative areas in C9-ALS patients, indicating that DPRs may exert cell non-autonomous effects, in addition to the known intracellular pathological mechanisms. Here, we report that poly-GA, the most abundant form of DPR in C9-ALS, is released from cells. Local administration of poly-GA proteins in peripheral synaptic regions causes muscle weakness and impaired neuromuscular transmission *in vivo*. The NMJ structure cannot be maintained, as evidenced by the fragmentation of postsynaptic acetylcholine receptor (AChR) clusters and distortion of presynaptic nerve terminals. Mechanistic study demonstrated that extracellular poly-GA sequesters soluble Agrin ligands and inhibits Agrin-MuSK signaling. Our findings provide a novel cell non-autonomous mechanism by which poly-GA impairs NMJs in C9-ALS. Thus, targeting NMJs could be an early therapeutic intervention for C9-ALS.

Keywords: Amyotrophic lateral sclerosis; Neuromuscular junction; Poly-Gly-Ala; Agrin

INTRODUCTION

Amyotrophic lateral sclerosis (ALS) is a devastating motoneuron disorder that affects approximately five in every 100 000 people across various populations. Degenerated motoneurons lose control of skeletal muscles and ALS patients rapidly exhibit progressive muscle atrophy, paralysis, and breathing failure, eventually dying within ~5 years of onset (Gendron et al., 2017). To date, there is no effective treatment for the disorder, partly because of our incomplete understanding of the causative pathological mechanisms. One postulated theory, referred to as the “dying-back” hypothesis, suggests that the destabilization of the neuromuscular junction (NMJ), the synaptic connection between motoneurons and skeletal muscle fibers, may represent an early event in the progression of ALS (Geevasinga et al., 2016; Moloney et al., 2014). This hypothesis posits that the distal end of the motor axon terminal is particularly vulnerable, with synaptic function and structure being susceptible to defects prior to the loss of the motoneuron cell body (Chand et al., 2018; Geevasinga et al., 2016; Moloney et al., 2014).

As a cholinergic synapse, the NMJ rapidly conveys signals from motoneurons to muscle fibers to control motor behaviors (Li et al., 2018; Shen et al., 2015; Wu et al., 2010). Motor nerve terminals release acetylcholine (ACh) to activate ACh receptors (AChRs) on muscle fibers. The clustering of postsynaptic AChRs (density of approximately 12 000 molecules per μm^2) is regulated by the Agrin-LRP4-MuSK complex (Li et al., 2018; Shen et al., 2015; Wu et al., 2010). Agrin is an extracellular matrix protein belonging to the heparan sulfate proteoglycan family (Bezakova & Ruegg, 2003). Neuronal Agrin originating from nerve terminals activates the tyrosine kinase receptor MuSK with the aid of its co-receptor LRP4 in muscle fibers (Kim et al., 2008; Zhang et al., 2008). MuSK activation triggers a cascade of events that culminate in the clustering of AChRs. Disruption of Agrin signaling impairs the structure and function of NMJs and causes neuromuscular disorders including myasthenia gravis (MG) and ALS (Shen et al., 2015). Mutations in NMJ genes or autoantibodies against NMJ proteins have been identified in patients with congenital myasthenic syndrome (CMS), MG, and/or ALS (Gilhus et al., 2016; Rivner et al., 2017; Rodriguez Cruz et al., 2014; Shen et al., 2015; Tzartos et al., 2014). Agrin signal enhancement rescues ALS, CMS, spinal

Received: 14 December 2022; Accepted: 15 February 2023; Online: 17 February 2023

Foundation items: This work was supported by the National Key Research and Development Program of China (2022YFF1000500 to K.Z. and 2021YFA1101100 to C.S.), Zhejiang Provincial Natural Science Foundation (LZ22C110002 to C.S.), and National Natural Science Foundation of China (32271031 to K.Z. and 82230038, 31871203, and 32071032 to C.S.)

[#]Authors contributed equally to this work

*Corresponding authors, E-mail: cshen@zju.edu.cn; kjzhang@zju.edu.cn

muscular atrophy (SMA), and muscular dystrophy (MD) in animal models (Arimura et al., 2014; Bentzinger et al., 2005; Hettwer et al., 2014; Miyoshi et al., 2017; Perez-Garcia & Burden, 2012), indicating that the NMJ may be a therapeutic target for neuromuscular disorders (Ohno et al., 2017).

The excessive expansion of GGGGCC (G4C2) repeats in the *c9orf72* gene is considered a leading genetic cause of ALS and frontotemporal dementia (FTD) (Dejesus-Hernandez et al., 2011; Renton et al., 2011). Multiple G4C2 RNA foci have been detected in the spinal cord of C9-ALS patients (Dejesus-Hernandez et al., 2011). Studies conducted in flies and mice have demonstrated impairments in the structure and function of the NMJ in the presence of G4C2 repeats (Freibaum et al., 2015; Herranz-Martin et al., 2017; Liu et al., 2016; Zhang et al., 2015). The pathological mechanisms underlying C9-ALS have been linked to dipeptide repeat proteins (DPRs) that result from G4C2 repeat-associated non-ATG translation (RAN) (Gao et al., 2017b; O'rourke et al., 2016; Taylor et al., 2016). Poly-GA is the most abundant C9-DPR species detected in the brains of C9-ALS/FTD patients (Mackenzie et al., 2013; Mori et al., 2013). Importantly, the tendency of poly-GA to form protein aggregates and elicit neurotoxicity mimics the neurocytoplasmic inclusions seen in neurodegenerative disorders, suggesting that poly-GA is a driving force of DPR neurotoxicity during chronic motoneuron degeneration (Lee et al., 2017; May et al., 2014; Schludi et al., 2015; Yamakawa et al., 2015; Zhang et al., 2016a). We recently reported that the intraneuronal UBQLN2-HSP70 axis facilitates poly-GA clearance and that disruption of this process contributes to ALS pathogenesis (Zhang et al., 2021). The toxic effects of DPR proteins, including nucleolar stress, nucleocytoplasmic transport defects, and proteasomal dysfunction, have been demonstrated in prior studies (Gao et al., 2017a; Haeusler et al., 2016; Taylor et al., 2016). Notably, as these effects occur intracellularly, DPR proteins are believed to function in a cell-autonomous manner (Gao et al., 2017a; Taylor et al., 2016).

Poly-GA has been detected in cultured cell medium (Westergard et al., 2016; Zhou et al., 2017b) and cerebrospinal fluid (CSF) of C9-ALS patients (Krishnan et al., 2022). Co-culture assays have shown that poly-GA proteins can be released and transferred between cells to cause toxicity (Westergard et al., 2016; Zhou et al., 2017b). Antibodies against poly-GA can mitigate motor defects in C9-ALS mice, suggesting that extracellular poly-GA proteins may play critical roles in ALS pathogenesis (Nguyen et al., 2020). However, the potential occurrence and mechanism by which extracellular poly-GA proteins regulate synaptic transmission between motoneurons and skeletal muscles remain largely unknown.

In the current study, we found that local administration of poly-GA in peripheral synaptic regions caused muscle weakness and impaired neuromuscular synaptic transmission. Mechanistic studies indicated that extracellular poly-GA sequestered the soluble Agrin ligand and inhibited Agrin-induced AChR clustering in cultured myotubes. Thus, our study identified a novel pathological mechanism for C9-ALS.

MATERIALS AND METHODS

Animals

All male mice (C57BL/6J background) used in this study were raised in standard conditions under a 12 h light-dark cycle with free access to food and water. All animal experiments were approved by the Institutional Animal Care and Use Committee of Zhejiang University (Approval No.: 12306).

Western blot analysis

Western blotting was performed as described previously (Shen et al., 2008). For the detection of C9-DPR proteins in the cell medium, N2a cells were transfected with $(G4C2)_{50}$-Flag-pcDNA3 plasmids using Lipo2000 (ThermoFisher Scientific, USA). After 48 h, the cell medium was replaced with 0.5% fetal bovine serum (FBS)/Dulbecco's Modified Eagle Medium (DMEM) for 8 h. Conditioned cell medium was centrifuged at 5 000 ×*g* for 5 min at 4 °C to remove cell debris, concentrated using a Centricon-YM3 column, and subjected to immunoblot analysis. To detect insoluble poly-GA protein aggregates, poly-GA was resolved by sodium dodecyl-sulfate polyacrylamide gel electrophoresis (SDS-PAGE), and the stacking gel was transferred onto a polyvinylidene fluoride (PVDF) membrane for immunoblotting. To detect phospho-MuSK (pMuSK) in cultured cells, C2C12 myotubes were pretreated with poly-GA for 3 h, followed by stimulation with Agrin for 30 min. Cells were lysed in modified RIPA buffer (50 mmol/L Tris-HCl, pH 7.4; 150 mmol/L NaCl; 1% NP-40; 0.5% TritonX-100; 1 mmol/L PMSF; 1 mmol/L EDTA; 5 mmol/L NaF; 2 mmol/L Na_3VO_4; and protease inhibitors). The resulting lysates (60 μg of protein) were subjected to immunoblotting. For *in vivo* detection of pMuSK, tibialis anterior (TA) muscles were homogenized with RIPA buffer (1:50 mg/μL), and the resulting lysate supernatants (60 μg of protein) were subjected to immunoblotting.

The primary antibodies used for western blotting were: anti-pMuSK (1:1 000; D151396; Sangon Biotech, China), anti-MuSK (1:1 000; home-made) (Shen et al., 2013), anti-α-tubulin (1:3 000; sc-23948; Santa Cruz, USA), anti-Flag (1:2 000; F7425; Sigma-Aldrich, USA), and anti-His (1:1 000; D152405; Sangon Biotech, China). Horseradish peroxidase (HRP)-conjugated goat anti-mouse and rabbit immunoglobulin G (IgG) antibodies were obtained from ThermoFisher (1:5 000; 31430; 1460, USA). Immunoreactive bands were visualized using a SuperSignal West Femto Maximum Sensitivity Substrate (ThermoFisher, USA). Immunoblot images were analyzed with ImageJ.

Purification of recombinant poly-GA proteins

For the expression of recombinant poly-GA proteins, G4C2 repeats (kindly provided by Dr. Taylor Paul from St. Jude Children's Research Hospital, USA) were inserted into a pFlag-CMV vector (pFlag-GA_{50}-His-CMV) containing an ATG start codon and artificial signal peptide to facilitate the expression and secretion of poly-GA, and a His tag at the C terminus to facilitate Ni-NTA column purification. Poly-GA proteins were purified as described previously (Shen et al., 2013). Briefly, N2a cells at 70% confluence were transfected with the empty vector or pFlag-GA_{50}-His-CMV using Lipo2000. After 48 h, the cell medium was replaced with 0.5% FBS/DMEM for 8 h. Conditioned medium of control or poly-GA-expressed cells was centrifuged at 5 000 ×*g* for 5 min at 4 °C to remove cell debris, and the supernatants were then mixed with BeyoGold™ His-tag purification resin (4% of cell medium volume, Beyotime Biotechnology, China) pre-equilibrated in 0.5% FBS/DMEM medium. The mixture was incubated at 4 °C overnight on a rotator. After the samples were loaded in gravity-flow columns, beads were washed five times with 10 bed volumes of washing buffer. Poly-GA was

eluted with 3 bed volumes of elution buffer, and different fractions were pooled together and dialyzed in cold phosphate-buffered saline (PBS) overnight. Poly-GA was further concentrated through a Centricon-YM3 column (Millipore, USA) and quantified using the Bradford assay. The same amount of bovine serum albumin (BSA) was added to the control solution. The purity of poly-GA was confirmed by western blot analysis with an anti-Flag antibody.

Local administration of poly-GA

Poly-GA (5 ng/μL in PBS, 20 μL) was injected into the center of the TA muscle in one hindlimb of 8-week-old male C57/B6J mice. To reduce variability among mice, the corresponding TA muscle in the opposite hindlimb of each mouse was injected with the same volume of PBS or BSA (5 ng/μL, 20 μL) as a control. The injections were repeated every three days and the mice subjected to blinded behavioral and electromyography analyses 30 days later.

Measurement of grip strength

Grip strength was assessed using a rodent grasping force measuring instrument (YLS-13A, Shandong Academy of Medical Sciences, China) as described previously (Xiao et al., 2020). To measure grip strength of the GA-injected hindlimb, the other three feet were secured using soft tape. The mice were held by their tail, allowed to grip a grid connected to a scale, then gently pulled in the horizontal direction until the grip was released. The top five grip strength values of 10 consecutive trials were recorded.

Foot fault test

The foot fault test was conducted as described previously with minor modifications (Li et al., 2018; Zhou et al., 2017a). In brief, the mice were evaluated for hindlimb movement while walking on elevated metal grids with regularly placed bars (0.8 cm spacing). The instances in which the hindlimb fell or slipped between the bars were recorded as foot faults. The total number of hindlimb steps and total number of foot faults were recorded and the percentage of hindlimb foot faults to total steps within 5 min was calculated. Each mouse was required to cross the metal grids three times, with a 15 min rest period between each trial.

Electromyography

Mice were anesthetized with isoflurane (RWD Life Science, China). A stimulation needle electrode (092-DMF25-S; TECA, USA) was inserted near the sciatic nerve in the thigh of GA-injected and control mice. The reference needle electrode was inserted near the Achilles tendon, and the recording needle electrode was inserted in the middle of the TA muscle of the GA-injected or control legs (Shen et al., 2018). Reference and recording electrodes were connected to an Axopatch 200B amplifier (Molecular Devices, USA). Supramaximal stimulation was applied to the sciatic nerve for 10 stimulations at 1, 2, 5, 10, 20, and 30 Hz (30 s pause between trains). Compound muscle action potentials (CMAPs) were collected with a Digidata 1550A (Molecular Devices, USA). Peak-to-peak amplitudes were analyzed in Clampfit10.5 (Molecular Devices, USA).

Light microscopy analysis of NMJs

Whole-mount staining of TA muscles was performed as described previously (Shen et al., 2018; Tu et al., 2021). TA muscles of GA-injected mice were fixed in 4% paraformaldehyde (PFA) for 1 h and permeabilized for 2 h in 0.5% TritonX-100/PBS. Muscles were teased into fibers and incubated at 4 °C overnight with a mixture of R-BTX (1:2 000) and primary antibodies. After the tissues were washed with PBS three times, muscle fibers were incubated with goat anti-mouse/rabbit IgG conjugated with Alexa Fluor 488 (1:750; A-11029, A-11034; ThermoFisher, USA) for 2 h at room temperature. Images were obtained with a Nikon confocal microscope and analyzed with ImageJ. The following primary antibodies were used for immunostaining: anti-neurofilament (anti-NF, 1:1 000; 2837S; Cell Signaling Technology, USA), anti-SV2 (1:1 000; SV2; Developmental Studies Hybridoma Bank, USA), and anti-Flag (1:1 000; F7425; Sigma-Aldrich, USA).

Agrin-induced AChR clustering in C2C12 myotubes

AChR clusters were assayed as described previously with minor modifications (Chen et al., 2020; Zhang et al., 2014). C2C12 myotubes were pretreated with poly-GA (0.5, 5, and 50 ng/mL) followed by Agrin (1 nmol/L) for 16 h. After fixation in 4% PFA, cells were incubated with R-BTX (1:2 000) to label AChR clusters. Myotubes were viewed using a Leica fluorescence microscope, and AChR clusters (diameter or axis >4 μm) were scored. At least 10 views per dish in at least two dishes were scored in three independent experiments.

MTT assay

Cell viability was analyzed using the MTT (3-(4,5-dimethylthiazol-2-yl)-2,5- diphenyltetrazolium bromide) assay (Beyotime Biotechnology, China). Briefly, C2C12 myotubes in 12-well plates were treated with poly-GA (5 ng/mL) for 3 h. The MTT solution (5 mg/mL, 100 μL) was incubated with the cell medium for 4 h at 37 °C until purple pellets were seen in the plate. Formazan solution (800 μL) was added for another 4 h to dissolve the pellets. Absorbance was measured at 570 nm.

Mass spectrometry (MS) analysis

Intracerebroventricular AAV2/8 virus injections were administered in the brains of neonatal mice as described previously (Zhang et al., 2021). In brief, C57BL/6 neonatal pups (P0) were cryoanesthetized on ice. In total, 2 μL of AAV2/8 (AAV-GFP or AAV-GFP-GA, 2.5×10^{12} vg/mL each) was slowly injected into the cerebral ventricles. The cortices were harvested at 3 months of age in lysis buffer containing 0.5% NP-40 and protease inhibitor cocktail. The lysates were centrifuged at 13 000 ×*g* for 15 min at 4 °C to remove debris, then incubated with GFP-conjugated beads overnight at 4 °C. The beads were washed three times with lysis buffer, and the bound proteins underwent MS analysis (PTM BioLabs, China).

Statistical analysis

The electromyography data were analyzed using two-way analysis of variance (ANOVA). Behavioral tests were analyzed by two-tailed paired Student's *t*-test. Western blots and images were analyzed using two-tailed unpaired Student's *t*-test. Unless otherwise indicated, data were expressed as the mean±standard error of the mean (*SEM*), and at least three independent experiments were performed. *P*-values of less than 0.05 were considered significant.

RESULTS

Poly-GA proteins impair motor functions and neurotransmission.

To better mimic the endogenous poly-GA proteins with no ATG translation initiation, we inserted $(G4C2)_{50}$ into the

pcDNA3 vector without ATG in the N-terminus. We added tag sequences to express Flag tag in open-reading frames of poly-GA (G4C2-Flag-pcDNA3). As expected, poly-GA-Flag was expressed in the total cell lysates (Figure 1A). Consistent with previous reports (Westergard et al., 2016; Zhou et al., 2017b), poly-GA proteins were present in the cell medium (Figure 1A). Whether extracellular poly-GA influences synapse functions *in vivo* is unknown. Thus, we transfected N2a cells with pFlag-GA_{50}-His-CMV plasmids that contain a signal peptide to facilitate the secretion of poly-GA. Poly-GA proteins were secreted in the conditioned cell medium (Figure 1B, lane 2). Extracellular poly-GA was further purified by affinity chromatography using Ni-NTA columns (Figure 1B, lanes 5 and 6).

Motoneurons innervate skeletal muscle and form NMJs at the surface of muscle fibers. We injected recombinant poly-GA proteins into the middle of mouse TA muscles where NMJs are enriched (Bai et al., 2022). To reduce background variation in different mice, we injected poly-GA in one hindlimb and injected the same volume of PBS in the other hindlimb of the same mouse as a control (Figure 1C; Supplementary Figure S1A). No differences in motor function or NMJ size were observed between the right and left hindlimbs (data not shown). Mice were injected every three days and subjected to behavioral analysis 30 days later. Strikingly, grip strength of the GA-injected hindlimbs was notably lower than that of the control hindlimbs (51.6±6.4 g in GA-injected mice vs. 83.8±9.2 g in PBS controls, n=11 mice, P<0.001; Figure 2D), indicating muscle weakness. The foot fault test showed that the percentage of foot faults during grid-walking was 58% higher in GA-injected hindlimbs compared to control limbs (158%±23% in GA-injected mice vs. 100%±22% in PBS controls, n=10 mice, P<0.001; Figure 2E).

To elucidate the pathological mechanisms underlying muscle weakness caused by GA-injection, electromyography was applied to assess potential impairment of neuromuscular transmission. CMAPs were measured in TA muscles in response to repetitive sciatic nerve stimulation (Shen et al., 2013; Zhao et al., 2017). In the control hindlimbs, CMAPs exhibited minimal variation after 10 consecutive nerve stimuli at different frequencies (Figure 2F). In contrast, CMAPs in the GA-injected muscles began to decrease from the 3rd stimulus and significantly decreased from the 7th (30 Hz) stimulus; the decrease in CMAP amplitude at the 10th stimulus was

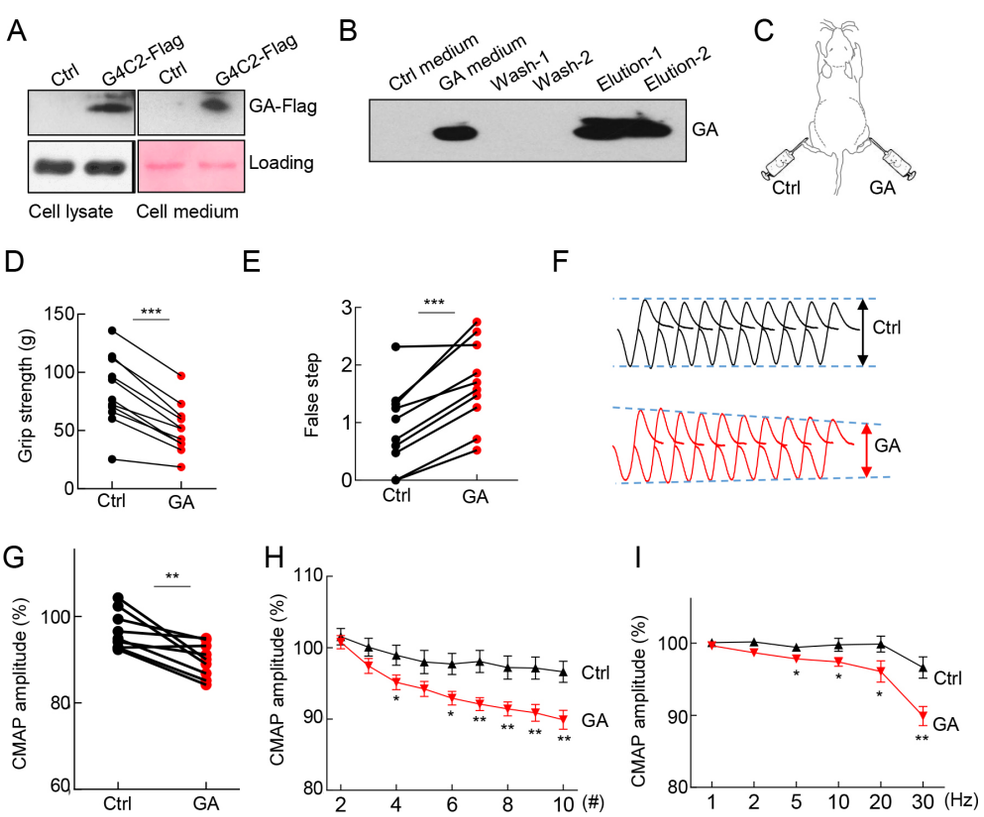

Figure 1 Poly-GA proteins impair motor function and neurotransmission

A: Conditioned medium of $(G4C2)_{50}$-Flag transfected cells was concentrated and subjected to immunoblot analysis. Poly-GA was detected in cell medium. B: Purification of poly-GA recombinant proteins with Ni-NTA columns. Conditioned medium of SP-Flag-GA-transfected cells was collected for purification. C: Diagram of local administration of poly-GA. Recombinant poly-GA proteins were injected into the middle of mouse tibialis anterior (TA) muscles where NMJs are enriched. To reduce background variation in different mice, poly-GA was injected into one hindlimb, and the same volume of PBS was injected in the other hindlimb in the same mouse. D: Grip strength of two hindlimbs of mice injected with control and poly-GA. n=11 mice, ***: P<0.001. E: Foot faults of two hindlimbs of mice injected with control and poly-GA. n=10 mice, ***: P<0.001. F: Ten CMAP traces were stacked in succession for better comparison. With successive stimulations, CMAP amplitude was reduced in GA-injected muscles. G: Reduced CMAP amplitudes in GA-injected muscles at 10th stimulation at 30 Hz. n=9 mice, **: P<0.01. H: Reduced CMAP amplitudes in GA-injected muscles at 10th stimulation at 30 Hz. n=9 mice, **: P<0.01. I: Reduction in CMAP amplitudes was stimulation frequency-dependent. n=9 mice, *: P<0.05; **: P<0.01. Unless otherwise specified, data are presented as mean±*SEM*. At least three independent experiments were performed. *: P<0.05; **: P<0.01; ***: P<0.001; ns: Not significant. Two-tailed paired Student's t-test in D, E, and G. Two-way ANOVA in H and I.

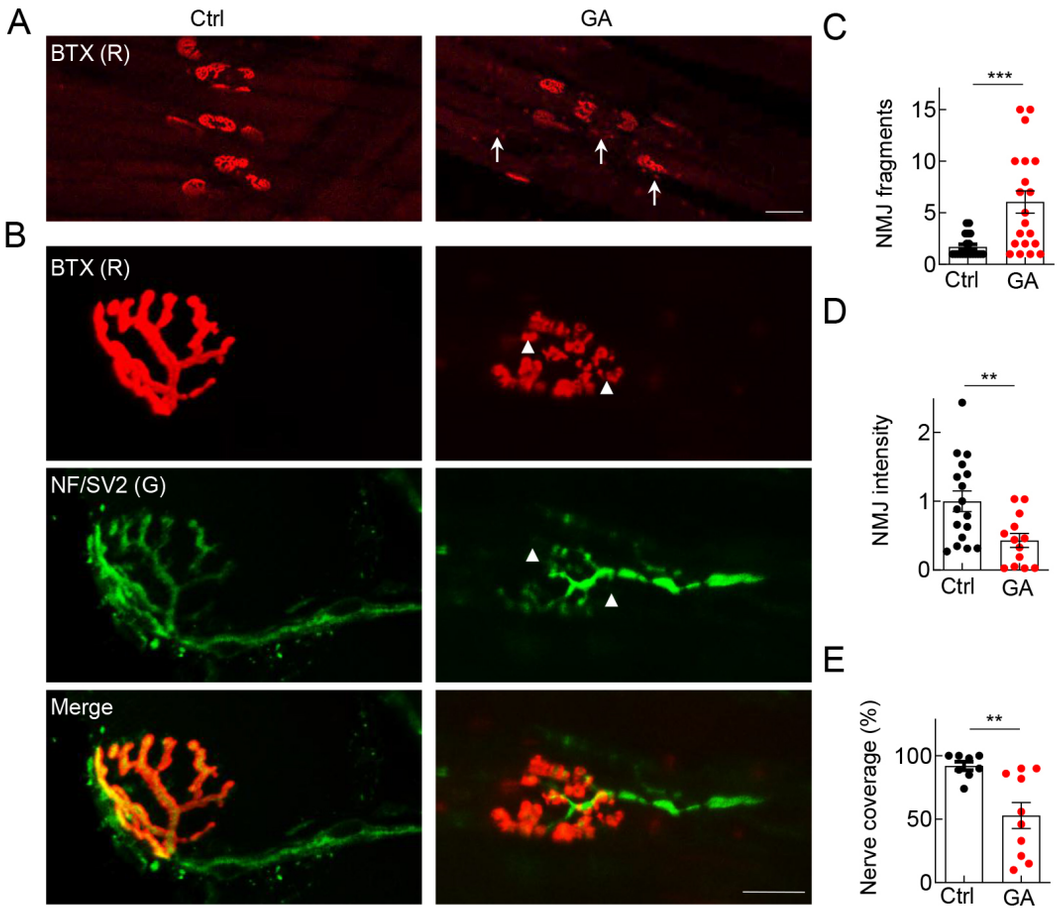

Figure 2 Poly-GA attenuates NMJ maintenance

A: TA muscle was whole-mount stained with R-BTX (red) to label AChRs. Scale bar: 50 μm. Broken NMJ fragments in GA-injected muscle are indicated by arrows. B: TA muscle was stained with R-BTX (red) to label AChR and antibodies against NF and SV2 (NF/SV2; green) to label nerve branches and terminals. Arrows indicate fragmented NMJs. Arrowheads indicate loss of nerve terminal coverage staining where R-BTX signal is positive. Scale bar: 10 μm. C: Quantitative analysis of AChR cluster fragments per NMJ. *n*=20 NMJs in poly-GA samples and *n*=20 NMJs in controls from three animals were analyzed. ***: *P*<0.001. D: Quantitative analysis of AChR intensity. *n*=13 NMJs in poly-GA samples and *n*=16 NMJs in controls from three animals were analyzed. **: *P*<0.01. E: Quantitative analysis of nerve coverage with AChR clusters. *n*=10 NMJs in poly-GA samples and *n*=8 NMJs in controls from three animals were analyzed. **: *P*<0.01. Unless otherwise specified, data are presented as mean±*SEM*. At least three independent experiments were performed. **: *P*<0.01; ***: *P*<0.001; Two-tailed unpaired Student's *t*-test in C, D, and E.

approximately 10% (Figure 2G, H). The reduction in CMAP amplitude in GA-injected hindlimbs was frequency-dependent and significant from 5 Hz to 30 Hz (Figure 2I), indicating a progressive loss of successful neuromuscular transmission after repeated stimulation. Collectively, these observations demonstrate that local administration of poly-GA impairs synaptic transmission and induces muscle weakness *in vivo*.

Poly-GA attenuates NMJ maintenance

The structural integrity of NMJs is crucial for ensuring the proper conveyance of nerve signals from presynaptic to postsynaptic regions. To determine whether poly-GA injection causes structural changes in NMJs, whole-mount TA muscles were stained with a mixture of R-BTX to label postsynaptic AChRs and antibodies against neurofilaments (NFs) and SV2 to label nerve branches and terminals (Shen et al., 2018). Subsequently, z-serial images were collected with confocal microscopy and collapsed into single images. In the control muscles, NMJs exhibited characteristic pretzel-like morphology, with complex continuous branches (Figure 2A, B). No inflammation was detected in either GA-injected or control muscles. However, the NMJs of GA-injected muscles were fragmented into many small pieces and showed a loss of connection between the AChR clusters (Figure 2A, B, arrow). The number of fragmented AChR clusters was 3.6-fold higher in GA-injected muscles than in the control group (6.05±1.09 vs. 1.70±0.24; *P*<0.001; Figure 2C). The intensity of R-BTX staining was significantly reduced in the GA-injected muscles (1.00±0.15 in controls vs. 0.43±0.10 in GA-injected mice; *P*<0.01; Figure 2D), suggesting dispersal of AChR clusters and a reduction in NMJ stability. Moreover, nerve fibers in control muscles were continuous, as evidenced by NF/SV2 staining, and the nerve terminal signal was well co-localized with the postsynaptic AChR pattern; in contrast, nerve fibers in the GA-injected muscles appeared disconnected and disorganized (Figure 2B, arrowhead). The AChR area covered by axon terminals was reduced from 92.0%±3.3% in control muscles to 52.9%±10.2% in GA-injected muscles (*P*<0.01; Figure 2E). Furthermore, some broken AChR clusters were located far from the NMJ regions but were still innervated, suggesting a reduction but not complete abolishment of NMJ functions in poly-GA-injected mice (Supplementary Figure S2).

NMJ defects are closely related to muscle injury. Indeed, we found a proportion of centralized nuclei in GA-injected muscles compared to control muscles (Supplementary Figure

S3A, B), although no differences in muscle fiber diameter (Supplementary Figure S3C). The use of BSA as a control confirmed that poly-GA proteins impaired motor functions (grip strength in Supplementary Figure S1B and foot steps in Supplementary Figure S1C) and synaptic transmission (CMAPs in Supplementary Figure S1D–G). No observable defects were present in the control muscles, suggesting that motor defects were primarily due to the poly-GA proteins rather than protein impurity. Together, these results indicate that poly-GA impairs neurotransmission, as demonstrated by the electrophysiological recordings (Figure 1).

Poly-GA inhibits Agrin-induced AChR clustering

We next investigated the cellular mechanisms by which extracellular poly-GA perturbs NMJ stability. Agrin binds to LRP4 to activate MuSK, thereby stimulating AChR clustering in muscle cells, which is considered critical for NMJ formation and maintenance *in vivo*. Having demonstrated a reduction in CMAP amplitude (Figure 1) and NMJ disassembly (Figure 2) in GA-injected muscles, we next sought to determine whether poly-GA impairs Agrin-induced AChR clustering in cultured C2C12 myotubes. As shown in Figure 3A, AChR clusters increased in response to Agrin stimulation, while pretreatment of poly-GA proteins in the medium significantly reduced Agrin-induced AChR clustering in a dose-dependent manner (Figure 3A, B). These results demonstrate that extracellular poly-GA may inhibit Agrin-induced AChR clustering in myotubes.

MuSK is phosphorylated at tyrosine 755 in response to Agrin stimulation, which is critical for the activation of the downstream signaling cascade (Burden et al., 2013). To investigate the underlying molecular mechanisms, we sought to determine whether extracellular poly-GA blocks Agrin-induced MuSK activation. C2C12 myotubes were pretreated with or without poly-GA before Agrin stimulation, and lysates were probed with an anti-pMuSK-specific antibody. In the controls, Agrin elicited MuSK tyrosine phosphorylation (Figure 3C, D). Poly-GA alone had little effect on the level of pMuSK, while Agrin-induced pMuSK was dramatically diminished by poly-GA pretreatment (Figure 3C, D). Total protein levels of MuSK remained consistent in the presence of poly-GA (Figure 3C, D). Importantly, pMuSK was reduced in the GA-injected muscle lysates (61.1%±8.8% vs. 100.0%±2.0% in controls, n=6, P<0.001; Figure 3F), while the total level of MuSK was sustained at a comparable level (Figure 3E). Taken together, these observations indicate that poly-GA can prevent Agrin from activating MuSK, thus explaining the inhibition of AChR clustering *in vitro* (Figure 3A) and NMJ disassembly *in vivo* (Figure 3).

Extracellular poly-GA sequesters Agrin

Previous studies have reported that poly-GA penetrates cells to promote the formation of RNA foci and seed aggregation of DPR proteins (Zhou et al., 2017b). However, we did not detect

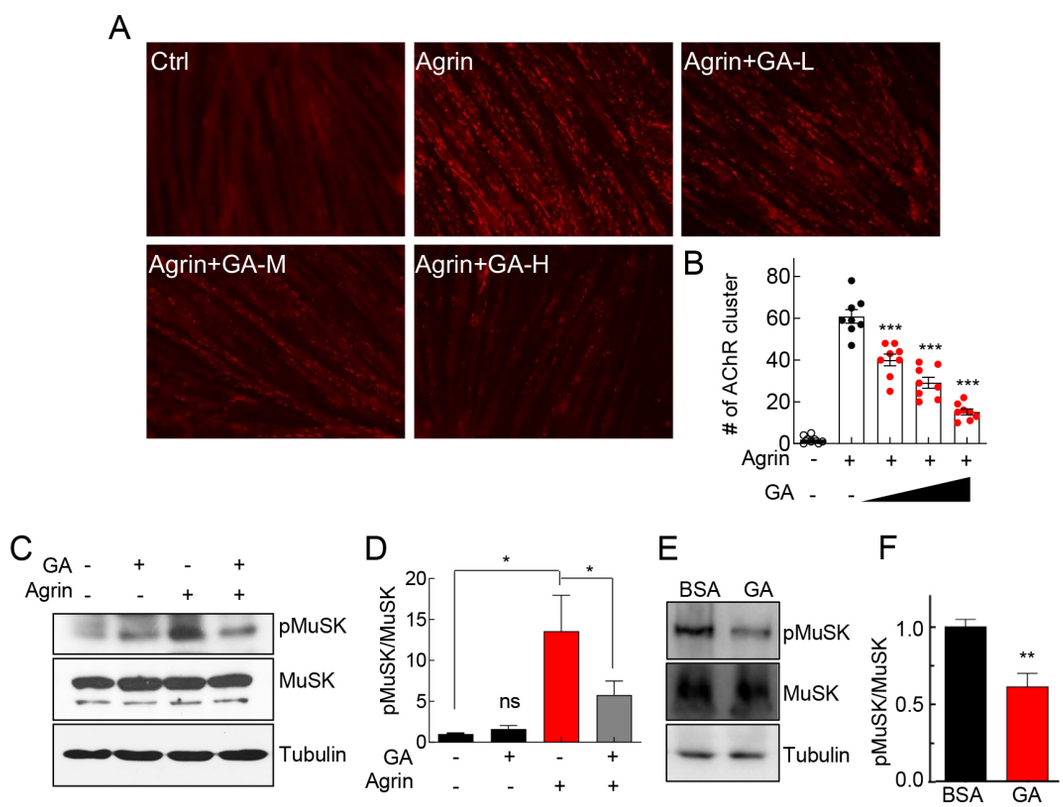

Figure 3 Poly-GA proteins inhibit Agrin-induced AChR clustering

A: C2C12 myotubes were incubated with or without Agrin for 8 h in the presence of different doses of poly-GA (GA-L, GA-M, GA-H). AChR clusters were visualized by R-BTX staining. B: Quantification of AChR clusters >4 μm in length from A. n=8 images in each group for statistics. ***: P<0.001. C: pMuSK and MuSK protein levels in GA-treated C2C12 myotubes. C2C12 was incubated with or without Agrin with poly-GA pretreatment. Cells were lysed and subjected to immunoblotting. D: Quantitative analysis of immunoblot in C. n=6 samples in each group. *: P<0.05. E: Immunoblots of pMuSK and MuSK in control and GA-injected muscles. F: Quantitative analysis of pMuSK/MuSK in E. n=6 samples in each group. ***: P<0.001. Unless otherwise specified, data are presented as mean±*SEM*. At least three independent experiments were performed. *: P<0.05; **: P<0.01, Two-tailed unpaired Student's t-test in F.

any difference in MTT values between the control and GA-treated myotubes (Figure 4A), excluding the possibility that inhibition of AChR clustering was caused by a GA-induced reduction in cell viability. We found that the injected poly-GA protein was enriched at NMJs, suggesting potential interaction between poly-GA and NMJ proteins (Figure 4B). We performed immunoprecipitation MS (IP-Mass) analysis using anti-GFP antibodies to pull down the GFP-GA protein complex in AAV-GFP-GA-injected mouse brains (Zhang et al., 2021), and identified neuronal Agrin as a GA-interacting protein. To determine whether poly-GA interferes with Agrin signaling by directly interacting with the extracellular Agrin ligand, we collected the conditioned cell medium of the Agrin-transfected N2a cells. Agrin proteins were pulled down by Myc antibody-conjugated agarose beads and were incubated with a poly-GA solution. We found that poly-GA was present in the same immunocomplex as Agrin but not in the control (Figure 4C).

Poly-GA peptides tend to form protein aggregates with β-sheet conformation in solution (Chang et al., 2016; Flores et al., 2016) and remain in stacking gels when resolved by SDS-PAGE (Zhang et al., 2016). Consistent with previous reports (Zhang et al., 2021), we detected insoluble GA in the stacking gel and soluble GA in the separating gel (Figure 4D). Interestingly, upon incubation with Agrin, there was more insoluble GA in the stacking gel, indicating that Agrin promoted poly-GA to form protein aggregates (285.3%±20.1% with Agrin vs. 100.0%±26.7% in controls, n=5, P<0.001; Figure 4D, F). Agrin also co-existed in the stacking gel with insoluble GA (Figure 4D), supporting interaction between Agrin and poly-GA (Figure 4C). Remarkably, the protein level of soluble Agrin in the separating gel was significantly reduced (100.0%±7.0% in control vs. 47.7%±9.7% with Agrin, n=5, P<0.01; Figure 4D, E). Taken together, our results suggest that extracellular poly-GA inhibits Agrin-MuSK signaling by sequestering the Agrin ligand.

DISCUSSION

NMJ degeneration occurs at the early stage of ALS. However, whether poly-GA of C9-ALS impairs synapse homeostasis is unknown. Here, we report that local administration of poly-GA at peripheral synaptic regions caused muscle weakness, impaired synaptic transmission, and destabilization of NMJ synapses. We further found that extracellular poly-GA sequestered soluble Agrin and inhibited Agrin-induced AChR clustering. Our study provides a novel pathological mechanism for poly-GA-mediated neurotoxicity in C9-ALS (Figure 5).

Cell non-autonomous effect of extracellular poly-GA

Microsatellite expansions in the genome have been implicated in several neurodegenerative diseases, including Huntington's disease (HD), spinocerebellar ataxia (SCA), myotonic

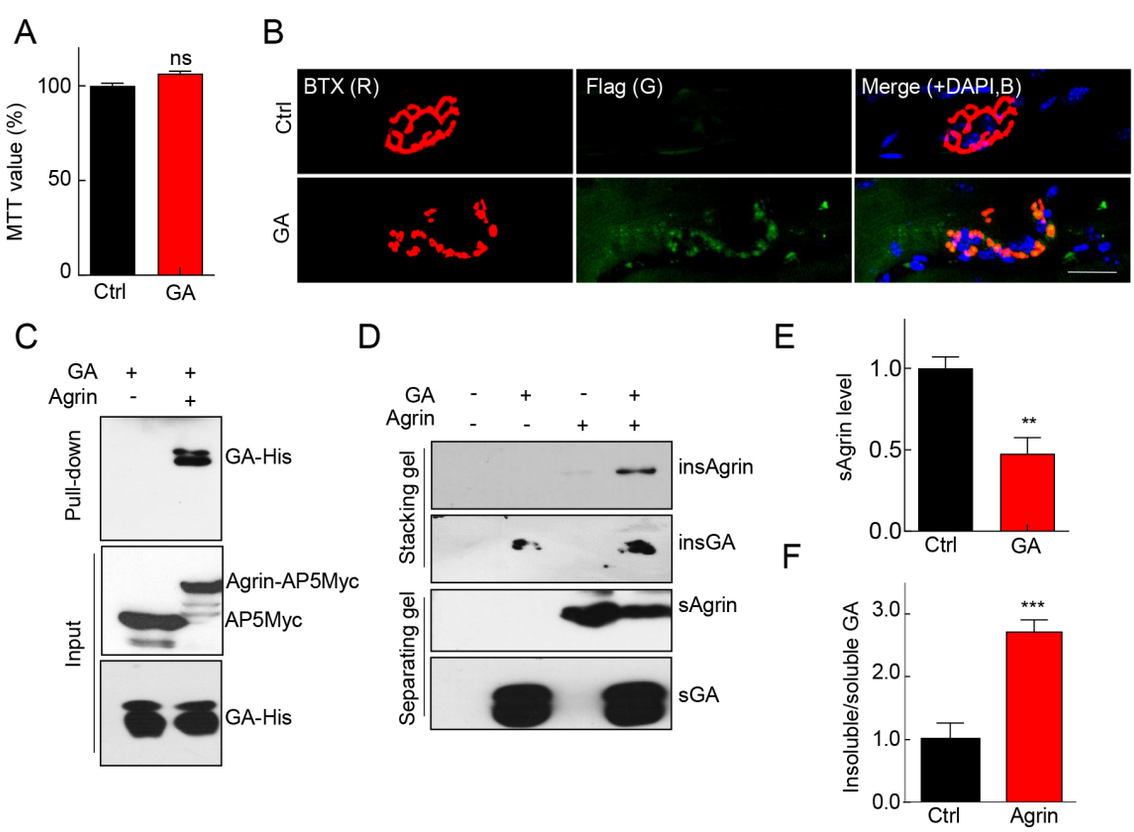

Figure 4 Extracellular poly-GA proteins sequester Agrin

A: MTT values in control and GA-treated C2C12 myotubes. ns: Not significant, P>0.05. B: Location of GA recombinant protein in GA-injected muscles. Anti-Flag, green; BTX, red; DAPI, blue. Scale bar: 10 μm. C: Poly-GA binding to Agrin. Agrin-AP5-Myc proteins in medium were immunoprecipitated by anti-Myc and incubated with poly-GA proteins. Poly-GA bound with Agrin but not with the control. D: GA sequesters soluble Agrin. When incubated with GA, Agrin in the stacking gel (insAgrin) increased, while Agrin in the separating gel (sAgrin) decreased. E, F: Quantitative analysis of sAgrin and insoluble GA in D. n=5 samples in each group. **: P<0.01; ***: P<0.001. Unless otherwise specified, data are presented as mean±*SEM*. At least three independent experiments were performed. **: P<0.01; ***: P<0.001, Two-tailed unpaired Student's t-test in E and F.

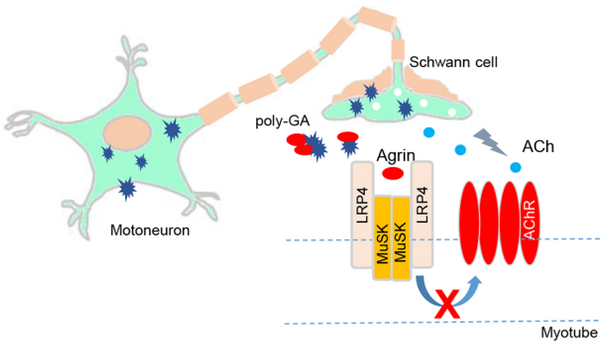

Figure 5 Proposed model

In the early stages of C9-ALS, poly-GA may be released from motoneuron terminals and sequester Agrin ligands to inhibit Agrin-induced AChR clustering, eventually causing NMJ disassembly, synaptic neurotransmission impairment, and muscle weakness.

dystrophy (MD), and C9-ALS (Cleary & Ranum, 2017). The discovery of RAN translation in 2011 changed our understanding of the underlying mechanisms of microsatellite expansion diseases (Zu et al., 2011). Most previous C9-ALS studies have focused on intracellular DPR proteins with cell-autonomous functions, such as nucleolar stress, nucleocytoplasmic transport defects, and proteasomal dysfunctions (Gao et al., 2017a; Haeusler et al., 2016; Taylor et al., 2016). However, no correlation has been found between the severity of DPR inclusion burdens and neurodegeneration in C9-ALS patients, except for poly-GR, suggesting there may be an additional cell non-autonomous effect of DPR proteins (Mackenzie et al., 2013; Saberi et al., 2018; Schludi et al., 2015). Poly-GA is the most abundant DPR species in the cerebellum of carriers of C9orf72 repeat expansion (Gendron et al., 2015). Poly-GA has also been detected in the CSF of C9-ALS patients (Krishnan et al., 2022) and can transfer between cells to spread toxicity in co-culture assays (Westergard et al., 2016; Zhou et al., 2017b). Antibodies against poly-GA can mitigate motor defects in C9-ALS mice, further suggesting that extracellular poly-GA proteins play critical roles in ALS pathogenesis (Nguyen et al., 2020). Here, we provide direct evidence that poly-GA proteins inhibit Agrin signaling and impair neuromuscular transmission *in vivo*, thus expanding our understanding of the pathological mechanisms of c9orf72-DPR proteins.

Synaptic regulation of extracellular poly-GA

Multiple G4C2 RNA foci have been detected in the spinal cord of C9-ALS patients (Dejesus-Hernandez et al., 2011), and NMJ function and structure are impaired in G4C2-overexpressed flies and mice (Freibaum et al., 2015; Herranz-Martin et al., 2017; Liu et al., 2016; Zhang et al., 2015). These observations suggest that peripheral synapses of lower motoneurons are damaged in C9-ALS. Our study revealed that recombinant GA proteins were accumulated at the NMJs (Figure 4), but cell viability was not reduced upon incubation with poly-GA in the cell medium of C2C12 myotubes (Figure 4), indicating that the GA-induced inhibitory effect on AChR clustering mainly occurred at the cell surface by blocking extracellular Agrin signaling, rather than functioning in myotubes through uptake. Proteomics results showed that poly-GA sequestered soluble Agrin and inhibited Agrin-MuSK signaling extracellularly (Figure 4). However, it is possible that poly-GA and Agrin interact intracellularly when both are expressed in motoneurons, and thus we cannot rule out the possibility that neuronal poly-GA may trigger the retention of Agrin inside motoneurons and reduce the secretion of Agrin at NMJs. As a component of extracellular matrix proteins, Agrin may promote poly-GA aggregation (Moretto et al., 2022), possibly related to heparan sulfate proteoglycans (Bezakova & Ruegg, 2003). In other neurodegenerative disorders, fibrils of α-synuclein, Aβ42, and HTTExon1 are transported along axons and secreted in medium without axon lysis (Brahic et al., 2016). Secreted Aβ can target many synaptic proteins and impair their functions. Poly-GA causes a reduction in presynaptic protein SV2 (Jensen et al., 2020). To the best of our knowledge, this is the first study to report that extracellular poly-GA regulates postsynaptic assembly. Furthermore, our study dissected the neurotoxic effects of DPR proteins from G4C2/C4G2-induced RNA foci, providing direct evidence that DPR proteins exhibit neuronal toxicity by targeting synapses.

Targeting NMJs as an early therapeutic intervention for ALS

Despite tremendous efforts, more than 50 clinical trials related to ALS treatment have failed, with only one minimally effective drug, riluzole, currently approved for clinical use (Gendron et al., 2017). These failures can partially be attributed to the delay in treating ALS patients, after motoneuronal cell bodies have already begun to degenerate (Bertrand et al., 2018). NMJ degeneration is believed to occur during the early stages of ALS, preceding the loss of motoneuronal cell bodies and the manifestation of clinical symptoms (Chand et al., 2018; Moloney et al., 2014). Poly-GA triggers motor deficits before neuronal loss in C9orf72 mouse models (Schludi et al., 2017). Dysfunctional NMJs impair neurotransmission between motoneurons and skeletal muscles, resulting in the destabilization of hypofunctional synapses and eventual death of motoneurons, starting from the nerve terminals (Moloney et al., 2014). Agrin signaling plays a critical role in NMJ formation and maintenance (Li et al., 2017; Wu et al., 2010) and its disruption results in impaired NMJ structure and function (Li et al., 2017), contributing to neuromuscular disorders, including ALS and MG. Autoantibodies against Agrin, LRP4, MuSK, or AChR have been identified in MG and ALS (Gilhus et al., 2016; Rivner et al., 2017; Tzartos et al., 2014). Mutations in the *AGRN*, *MuSK*, *LRP4*, and *DOK7* genes can also cause neuromuscular disorders such as CMS (Rodriguez Cruz et al., 2014; Shen et al., 2015). Thus, enhancing Agrin signaling to stabilize NMJs may offer therapeutic benefit for these diseases (Ohno et al., 2017). Our study suggests that targeting NMJs could serve as an early therapeutic intervention for ALS and other neuromuscular disorders. Future investigations will explore whether extracellular poly-GA impairs synapse neurotransmission in the central nervous system to elucidate the potential mechanisms of the cognitive defects observed in C9-ALS/FTD patients.

SUPPLEMENTARY DATA

Supplementary data to this article can be found online.

COMPETING INTERESTS

The authors declare that they have no competing interests.

AUTHORS' CONTRIBUTIONS

K.Z. and C.S.: Conceptualization, supervision, resources, and writing.

W.Y.T. and W.X.: Methodology, investigation, and writing. J.Z., S.Q., and L.B.: Investigation. All authors read and approved the final version of the manuscript.

REFERENCES

Arimura S, Okada T, Tezuka T, et al. 2014. *DOK7* gene therapy benefits mouse models of diseases characterized by defects in the neuromuscular junction. *Science*, **345**(6203): 1505−1508.

Bai L, Tu WY, Xiao YT, et al. 2022. Motoneurons innervation determines the distinct gene expressions in multinucleated myofibers. *Cell & Bioscience*, **12**(1): 140.

Bentzinger CF, Barzaghi P, Lin S, et al. 2005. Overexpression of mini-agrin in skeletal muscle increases muscle integrity and regenerative capacity in laminin-α2-deficient mice. *The FASEB Journal*, **19**(8): 934−942.

Bertrand A, Wen J, Rinaldi D, et al. 2018. Early cognitive, structural, and microstructural changes in presymptomatic *C9orf72* Carriers younger than 40 years. *JAMA Neurology*, **75**(2): 236−245.

Bezakova G, Ruegg MA. 2003. New insights into the roles of agrin. *Nature Reviews Molecular Cell Biology*, **4**(4): 295−309.

Brahic M, Bousset L, Bieri G, et al. 2016. Axonal transport and secretion of fibrillar forms of α-synuclein, Aβ42 peptide and HTTExon 1. *Acta Neuropathologica*, **131**(4): 539−548.

Burden SJ, Yumoto N, Zhang W. 2013. The role of MuSK in synapse formation and neuromuscular disease. *Cold Spring Harbor Perspectives in Biology*, **5**(5): a009167.

Chand KK, Lee KM, Lee JD, et al. 2018. Defects in synaptic transmission at the neuromuscular junction precede motor deficits in a TDP-43^{Q331K} transgenic mouse model of amyotrophic lateral sclerosis. *The FASEB Journal*, **32**(5): 2676−2689.

Chang YJ, Jeng US, Chiang YL, et al. 2016. The glycine-alanine dipeptide repeat from C9orf72 hexanucleotide expansions forms toxic amyloids possessing cell-to-cell transmission properties. *Journal of Biological Chemistry*, **291**(10): 4903−4911.

Chen AZ, Bai L, Zhong KK, et al. 2020. APC2^{CDH1} negatively regulates agrin signaling by promoting the ubiquitination and proteolytic degradation of DOK7. *The FASEB Journal*, **34**(9): 12009−12023.

Cleary JD, Ranum LPW. 2017. New developments in RAN translation: insights from multiple diseases. *Current Opinion in Genetics & Development*, **44**: 125−134.

DeJesus-Hernandez M, Mackenzie IR, Boeve BF, et al. 2011. Expanded GGGGCC hexanucleotide repeat in noncoding region of *C9ORF72* causes chromosome 9p-linked FTD and ALS. *Neuron*, **72**(2): 245−256.

Flores BN, Dulchavsky ME, Krans A, et al. 2016. Distinct *C9orf72*-associated dipeptide repeat structures correlate with neuronal toxicity. *PLoS One*, **11**(10): e0165084.

Freibaum BD, Lu YB, Lopez-Gonzalez R, et al. 2015. GGGGCC repeat expansion in *C9orf72* compromises nucleocytoplasmic transport. *Nature*, **525**(7567): 129−133.

Gao FB, Almeida S, Lopez-Gonzalez R. 2017a. Dysregulated molecular pathways in amyotrophic lateral sclerosis-frontotemporal dementia spectrum disorder. *The EMBO Journal*, **36**(20): 2931−2950.

Gao FB, Richter JD, Cleveland DW. 2017b. Rethinking unconventional translation in neurodegeneration. *Cell*, **171**(5): 994−1000.

Geevasinga N, Menon P, Özdinler PH, et al. 2016. Pathophysiological and diagnostic implications of cortical dysfunction in ALS. *Nature Reviews Neurology*, **12**(11): 651−661.

Gendron TF, Chew J, Stankowski JN, et al. 2017. Poly(GP) proteins are a useful pharmacodynamic marker for *C9ORF72*-associated amyotrophic lateral sclerosis. *Science Translational Medicine*, **9**(383): eaai7866.

Gendron TF, van Blitterswijk M, Bieniek KF, et al. 2015. Cerebellar c9RAN proteins associate with clinical and neuropathological characteristics of *C9ORF72* repeat expansion carriers. *Acta Neuropathologica*, **130**(4): 559−573.

Gilhus NE, Skeie GO, Romi F, et al. 2016. Myasthenia gravis - autoantibody characteristics and their implications for therapy. *Nature Reviews Neurology*, **12**(5): 259−268.

Haeusler AR, Donnelly CJ, Rothstein JD. 2016. The expanding biology of the *C9orf72* nucleotide repeat expansion in neurodegenerative disease. *Nature Reviews Neuroscience*, **17**(6): 383−395.

Herranz-Martin S, Chandran J, Lewis K, et al. 2017. Viral delivery of *C9orf72* hexanucleotide repeat expansions in mice leads to repeat-length-dependent neuropathology and behavioural deficits. *Disease Models & Mechanisms*, **10**(7): 859−868.

Hettwer S, Lin S, Kucsera S, et al. 2014. Injection of a soluble fragment of neural agrin (NT-1654) considerably improves the muscle pathology caused by the disassembly of the neuromuscular junction. *PLoS One*, **9**(2): e88739.

Jensen BK, Schuldi MH, McAvoy K, et al. 2020. Synaptic dysfunction induced by glycine-alanine dipeptides in C9orf72-ALS/FTD is rescued by SV2 replenishment. *EMBO Molecular Medicine*, **12**(5): e10722.

Kim N, Stiegler AL, Cameron TO, et al. 2008. Lrp4 is a receptor for Agrin and forms a complex with MuSK. *Cell*, **135**(2): 334−342.

Krishnan G, Raitcheva D, Bartlett D, et al. 2022. Poly(GR) and poly(GA) in cerebrospinal fluid as potential biomarkers for *C9ORF72*-ALS/FTD. *Nature Communications*, **13**(1): 2799.

Lee YB, Baskaran P, Gomez-Deza J, et al. 2017. C9orf72 poly GA RAN-translated protein plays a key role in amyotrophic lateral sclerosis via aggregation and toxicity. *Human Molecular Genetics*, **26**(24): 4765−4777.

Li L, Xiong WC, Mei L. 2018. Neuromuscular junction formation, aging, and disorders. *Annual Review of Physiology*, **80**: 159−188.

Li WY, Wang Y, Zhai FG, et al. 2017. AAV-KLF7 promotes descending propriospinal neuron axonal plasticity after spinal cord injury. *Neural Plasticity*, **2017**: 1621629.

Liu YJ, Pattamatta A, Zu T, et al. 2016. *C9orf72* BAC mouse model with motor deficits and neurodegenerative features of ALS/FTD. *Neuron*, **90**(3): 521−534.

Mackenzie IR, Arzberger T, Kremmer E, et al. 2013. Dipeptide repeat protein pathology in *C9ORF72* mutation cases: clinico-pathological correlations. *Acta Neuropathologica*, **126**(6): 859−879.

May S, Hornburg D, Schludi MH, et al. 2014. C9orf72 FTLD/ALS-associated Gly-Ala dipeptide repeat proteins cause neuronal toxicity and Unc119 sequestration. *Acta Neuropathologica*, **128**(4): 485−503.

Miyoshi S, Tezuka T, Arimura S, et al. 2017. *DOK7* gene therapy enhances motor activity and life span in ALS model mice. *EMBO Molecular Medicine*, **9**(7): 880−889.

Moloney EB, De Winter F, Verhaagen J. 2014. ALS as a distal axonopathy: molecular mechanisms affecting neuromuscular junction stability in the presymptomatic stages of the disease. *Frontiers in Neuroscience*, **8**: 252.

Moretto E, Stuart S, Surana S, et al. 2022. The role of extracellular matrix components in the spreading of pathological protein aggregates. *Frontiers in Cellular Neuroscience*, **16**: 844211.

Mori K, Weng SM, Arzberger T, et al. 2013. The *C9orf72* GGGGCC repeat is translated into aggregating dipeptide-repeat proteins in FTLD/ALS. *Science*, **339**(6125): 1335−1338.

Nguyen L, Montrasio F, Pattamatta A, et al. 2020. Antibody therapy targeting RAN proteins rescues C9 ALS/FTD phenotypes in *C9orf72* mouse model. *Neuron*, **105**(4): 645−662.e11.

Ohno K, Ohkawara B, Ito M. 2017. Agrin-LRP4-MuSK signaling as a therapeutic target for myasthenia gravis and other neuromuscular disorders. *Expert Opinion on Therapeutic Targets*, **21**(10): 949−958.

O'Rourke JG, Bogdanik L, Yáñez A, et al. 2016. *C9orf72* is required for proper macrophage and microglial function in mice. *Science*, **351**(6279): 1324−1329.

Pérez-García MJ, Burden SJ. 2012. Increasing MuSK activity delays denervation and improves motor function in ALS mice. *Cell Reports*, **2**(3): 497−502.

Renton AE, Majounie E, Waite A, et al. 2011. A hexanucleotide repeat expansion in *C9ORF72* is the cause of chromosome 9p21-linked ALS-FTD. *Neuron*, **72**(2): 257−268.

Rivner MH, Liu SY, Quarles B, et al. 2017. Agrin and low-density lipoprotein-related receptor protein 4 antibodies in amyotrophic lateral sclerosis patients. *Muscle & Nerve*, **55**(3): 430−432.

Rodriguez Cruz PM, Palace J, Beeson D. 2014. Congenital myasthenic syndromes and the neuromuscular junction. *Current Opinion in Neurology*, **27**(5): 566−575.

Saberi S, Stauffer JE, Jiang J, et al. 2018. Sense-encoded poly-GR dipeptide repeat proteins correlate to neurodegeneration and uniquely co-localize with TDP-43 in dendrites of repeat-expanded C9orf72 amyotrophic lateral sclerosis. *Acta Neuropathologica*, **135**(3): 459−474.

Schludi MH, Becker L, Garrett L, et al. 2017. Spinal poly-GA inclusions in a *C9orf72* mouse model trigger motor deficits and inflammation without neuron loss. *Acta Neuropathologica*, **134**(2): 241−254.

Schludi MH, May S, Grässer FA, et al. 2015. Distribution of dipeptide repeat proteins in cellular models and *C9orf72* mutation cases suggests link to transcriptional silencing. *Acta Neuropathologica*, **130**(4): 537−555.

Shen CY, Chen YF, Liu HQ, et al. 2008. Hydrogen peroxide promotes Aβ production through JNK-dependent activation of γ-secretase. *Journal of Biological Chemistry*, **283**(25): 17721−17730.

Shen CY, Li L, Zhao K, et al. 2018. Motoneuron Wnts regulate neuromuscular junction development. *eLife*, **7**: e34625.

Shen CY, Lu YS, Zhang B, et al. 2013. Antibodies against low-density lipoprotein receptor-related protein 4 induce myasthenia gravis. *The Journal of Clinical Investigation*, **123**(12): 5190−5202.

Shen CY, Xiong WC, Mei L. 2015. LRP4 in neuromuscular junction and bone development and diseases. *Bone*, **80**: 101−108.

Taylor JP, Brown RH Jr, Cleveland DW. 2016. Decoding ALS: from genes to mechanism. *Nature*, **539**(7628): 197−206.

Tu WY, Xu WT, Zhang KJ, et al. 2021. Whole-mount staining of neuromuscular junctions in adult mouse diaphragms with a sandwich-like apparatus. *Journal of Neuroscience Methods*, **350**: 109016.

Tzartos JS, Zisimopoulou P, Rentzos M, et al. 2014. LRP4 antibodies in serum and CSF from amyotrophic lateral sclerosis patients. *Annals of Clinical and Translational Neurology*, **1**(2): 80−87.

Westergard T, Jensen BK, Wen XM, et al. 2016. Cell-to-cell transmission of dipeptide repeat proteins linked to *C9orf72*-ALS/FTD. *Cell Reports*, **17**(3): 645−652.

Wu HT, Xiong WC, Mei L. 2010. To build a synapse: signaling pathways in neuromuscular junction assembly. *Development*, **137**(7): 1017−1033.

Xiao YT, Zhang JM, Shu XQ, et al. 2020. Loss of mitochondrial protein CHCHD10 in skeletal muscle causes neuromuscular junction impairment. *Human Molecular Genetics*, **29**(11): 1784−1796.

Yamakawa M, Ito D, Honda T,et al. 2015. Characterization of the dipeptide repeat protein in the molecular pathogenesis of c9FTD/ALS. *Human Molecular Genetics*, **24**(6): 1630−1645.

Zhang B, Luo SW, Wang Q, et al. 2008. LRP4 serves as a coreceptor of agrin. *Neuron*, **60**(2): 285−297.

Zhang B, Shen CY, Bealmear B, et al. 2014. Autoantibodies to agrin in myasthenia gravis patients. *PLoS One*, **9**(3): e91816.

Zhang K, Donnelly CJ, Haeusler AR, et al. 2015. The *C9orf72* repeat expansion disrupts nucleocytoplasmic transport. *Nature*, **525**(7567): 56−61.

Zhang KJ, Wang AL, Zhong KK, et al. 2021. UBQLN2-HSP70 axis reduces poly-Gly-Ala aggregates and alleviates behavioral defects in the *C9ORF72* animal model. *Neuron*, **109**(12): 1949−1962.e6.

Zhang YJ, Gendron TF, Grima JC, et al. 2016. *C9ORF72* poly(GA) aggregates sequester and impair HR23 and nucleocytoplasmic transport proteins. *Nature Neuroscience*, **19**(5): 668−677.

Zhao K, Shen CY, Lu YS, et al. 2017. Muscle yap is a regulator of neuromuscular junction formation and regeneration. *Journal of Neuroscience*, **37**(13): 3465−3477.

Zhou J, Li J, Rosenbaum DM, et al. 2017a. The prolyl 4-hydroxylase inhibitor GSK360A decreases post-stroke brain injury and sensory, motor, and cognitive behavioral deficits. *PLoS One*, **12**(9): e0184049.

Zhou QH, Lehmer C, Michaelsen M, et al. 2017b. Antibodies inhibit transmission and aggregation of *C9orf72* poly-GA dipeptide repeat proteins. *EMBO Molecular Medicine*, **9**(5): 687−702.

Zu T, Gibbens B, Doty NS, et al. 2011. Non-ATG-initiated translation directed by microsatellite expansions. *Proceedings of the National Academy of Sciences of the United States of America*, **108**(1): 260−265.